Achimer
http://archimer.ifremer.fr

Oyster reproduction is affected by exposure to polystyrene microplastics

Sussarellu Rossana [1], Suquet Marc [1], Thomas Yannick [1], Lambert Christophe [1], Fabioux Caroline [1], Pernet Marie Eve Julie [1], Le Goïc Nelly [1], Quillien Virgile [1], Mingant Christian [1], Epelboin Yanouk [1], Corporeau Charlotte [1], Guyomarch Julien [2], Robbens Johan [3], Paul-Pont Ika [1], Soudant Philippe [1], Huvet Arnaud [1, *]

[1] Laboratoire des Sciences de l'Environnement Marin, UMR 6539 UBO-CNRS-Institute Français de Recherche pour l'Exploitation de la Mer-Institute de Recherche pour le Développement, 29280 Plouzané, France
[2] Centre de Documentation de Recherche d'Expérimentations, 29218 Brest, France;
[3] Instituut poor Landbouw en Visserijonderzoek, 8400 Ostend, Belgium

* Corresponding author : Arnaud Huvet, tel. +33 (0)2 98 22 46 93 ;
email address : arnaud.huvet@ifremer.fr

Abstract :

Plastics are persistent synthetic polymers that accumulate as waste in the marine environment. Microplastic (MP) particles are derived from the breakdown of larger debris or can enter the environment as microscopic fragments. Because filter-feeder organisms ingest MP while feeding, they are likely to be impacted by MP pollution. To assess the impact of polystyrene microspheres (micro-PS) on the physiology of the Pacific oyster, adult oysters were experimentally exposed to virgin micro-PS (2 and 6 µm in diameter; 0.023 mg·L−1) for 2 mo during a reproductive cycle. Effects were investigated on ecophysiological parameters; cellular, transcriptomic, and proteomic responses; fecundity; and offspring development. Oysters preferentially ingested the 6-µm micro-PS over the 2-µm-diameter particles. Consumption of microalgae and absorption efficiency were significantly higher in exposed oysters, suggesting compensatory and physical effects on both digestive parameters. After 2 mo, exposed oysters had significant decreases in oocyte number (−38%), diameter (−5%), and sperm velocity (−23%). The D-larval yield and larval development of offspring derived from exposed parents decreased by 41% and 18%, respectively, compared with control offspring. Dynamic energy budget modeling, supported by transcriptomic profiles, suggested a significant shift of energy allocation from reproduction to structural growth, and elevated maintenance costs in exposed oysters, which is thought to be caused by interference with energy uptake. Molecular signatures of endocrine disruption were also revealed, but no endocrine disruptors were found in the biological samples. This study provides evidence that micro-PS cause feeding modifications and reproductive disruption in oysters, with significant impacts on offspring.

Keywords : microplastic, reproduction, energy allocation, oyster

Significance

Plastics are a contaminant of emerging concern accumulating in marine ecosystems. Plastics tend to break down into small particles, called microplastics, which also enter the marine environment directly as fragments from a variety of sources, including cosmetics, clothing, and industrial processes. Given their ubiquitous nature and small dimensions, the ingestion and impact of microplastics on marine life are a cause for concern, notably for filter feeders. Oysters were exposed to polystyrene microparticles, which were shown to interfere with energy uptake and allocation, reproduction, and offspring performance. A drop in energy allocation played a major role in this reproductive impairment. This study provides ground-breaking data on microplastic impacts in an invertebrate model, helping to predict ecological impact in marine ecosystems.

Introduction

Plastic production is continually increasing, with 299 million metric tons produced in 2013 and estimations of 33 billion tons for 2050 [1]. Plastic waste entering the oceans was calculated for 2010 at 4 to 12 million tons *per* year [2]. The consequences of macroplastic debris for wildlife are becoming well documented [3] Microplastic particles, defined as plastic particles smaller than 5 mm [4], derived from the fragmentation of larger debris [5, 6] or enter the environment directly as microscopic fragments [7]. MP pollution in the world's oceans has been recently estimated at over 5 trillion floating particles, corresponding to 250,000 tons [8].

Given the ubiquitous nature and small dimensions of MP [9], their ingestion and subsequent impact on marine life is a growing cause for concern, notably for suspension filter-feeding species, which filter large water volumes and may ingest large quantities of particles [10–13]. Effects of MP ingestion have already been studied in several filter-feeding species such as mussels [14–17], sea cucumbers [18], lungworms [13, 19], and some zooplankton [20–22]. These studies mainly showed a reduction of feeding activity [19], reserve depletion [13], inflammatory responses [15, 17] and translocation of MP into the circulatory system [14, 17]. Effects on fitness have been reported, with decreases in survival and fecundity in copepods [20, 22] and reproductive disruption in *Daphnia* [21]. At cellular and molecular levels, alterations of immunological responses, neurotoxic effects and the onset of genotoxicity have been observed in mussels exposed to PAH-contaminated polystyrene particles [17]. Additional impacts may arise from harmful plastic additives and/or persistent organic pollutants adsorbed on MP, which are known to be taken up and accumulated by living organisms [23].

In this study, the effects of MP exposure were assessed on reproductively active *Crassostrea gigas* adults and their offspring. The Pacific oyster was chosen because of its world-wide production, economic importance as seafood, and important role in estuarine and coastal habitats [24]. A two-month exposure of adult oysters to micro-sized polystyrene spheres (micro-PS, 2 and 6 μm, 0.023 mg L^{-1}) was performed under controlled conditions suitable for germ cell maturation. Polystyrene is one of the most commonly used plastic polymers worldwide, often found in microplastics sampled at sea [25, 26]. In our study, toxic endpoints were investigated through an integrative approach covering data from molecular and cellular parameters to ecophysiological behavior and energy budget modeling. Our results show that experimental micro-PS exposure on adult oysters affects feeding, absorption efficiency, gamete quality and fecundity, as well as impacting offspring growth.

Results

Ingestion and fate of micro-PS

Average daily ingestion of micro-PS particles was 14±2% of the 2-μm particles and 69±6% of the 6-μm particles supplied. From histological analysis micro-PS particles were only detected in the stomach and intestine (Figure 1) and did not reveal cellular inflammatory features in exposed animals.

Algal consumption, absorption efficiency and growth

Over the whole experiment, algal consumption was $4.30 \times 10^6 \pm 9.05 \times 10^5$ μm^3 of algae *per* oyster^{-1} h^{-1} with micro-PS and $4.26 \times 10^6 \pm 1.05$ μm^3 of algae *per* oyster^{-1} h^{-1} for the control. The two-way ANOVA revealed significantly higher algal consumption for exposed oysters (+3%, $p<0.01$), a significant date effect, and a date-exposure interaction ($p<0.001$). Absorption efficiency was 51.8±7.2% and 46.6±7.9% on average for micro-PS and control treatments, respectively. The two-way ANOVA revealed significantly higher absorption efficiency for exposed oysters (+11%, $p<0.01$). A significant date effect was observed ($p<0.001$). No significant difference in condition index was observed between exposed and control oysters (0.09±0.01 and 0.10±0.01, respectively).

Hemocyte counts and morphological and functional characteristics

Hyalinocytes and granulocytes were larger in exposed oysters (+6.7% and +16.1%, respectively) than in controls ($p<0.001$, Supplementary file 1). Significant interactions between date and exposure factors were found in oxidative activity for both hemocyte populations ($p<0.01$). The post-hoc test indicated that oxidative activity was higher in exposed oysters than in controls at T1 (+54% on average for both hemocyte types) and was lower at T2 (-31%) and T3 (-29.1%).

Reproduction, gamete quality and larval development

Histological examination at T3 revealed that all control and exposed oysters were in stage 3, corresponding to ripeness.

For females, the total number of oocytes collected by stripping and oocyte diameter were significantly lower in exposed females than controls (-38%, $p<0.01$ and -5%, $p<0.05$, respectively). Total numbers of oocytes were $2.3 \times 10^6 \pm 0.6$ for the exposed females and $3.8 \times 10^6 \pm 0.9$ for controls. Oocyte diameter

was 30.6±0.9 µm for exposed females and 32.2±1.1 µm for the control females. As an oocyte quality proxy, D-larval yield was estimated after making crosses by mixing oocytes collected from exposed and control females with control spermatozoa. A significant reduction in D-larval yield was observed in exposed females (29.6±0.3%) compared to control females (49.8±1.6%).

For males, significantly lower sperm velocity (-23%, *p*<0.05) was observed in exposed individuals (59.5±14.5 µm s^{-1}, *p*<0.05) compared with controls (77.5±9.3 µm s^{-1}). The percentage of motile sperm was similar between the two treatments, 40±16% and 51±11% for exposed and control males, respectively.

Finally, the larval growth was significantly slower (*p*<0.001, Figure 2) in progeny issued from exposed genitors than in progeny issued from control genitors. A mean reduction in size of 18.6% was observed at 17 days post fertilization: mean shell length was 279.8±12.5 µm for control progeny and 227.5±8.5 µm for progeny issued from exposed genitors, for which a 6-day lag in time to metamorphosis was observed.

Transcriptomic and proteomic analyses

In digestive gland, 76 transcripts were differentially expressed between exposed and control oysters (*p*<1.10^{-4}, FDR<5%, Supplementary file 2) and 1,266 transcripts were differentially expressed between sampling times T1 and T3 (*p*<0.01, FDR<5%). Two clusters of transcripts with similar expression patterns, down-regulated (cluster 1, n=51) and up-regulated (cluster 2, n=25), were revealed in exposed digestive glands compared with controls (Supplementary file 3). Response to glucocorticoid stimulus, fatty acid catabolic processes, respiratory burst and cellular response to mechanical stimulus were the main significantly enriched Gene Ontology (GO) biological processes.

In gonads, 46 transcripts were differentially expressed between exposed and control oysters (*p*<0.01, FDR<5%, Supplementary file 4), and 8,136 between the sampling time T1 and T3 (*p*<1.10^{-7}, FDR<5%). Two distinct clusters with similar expression patterns were found, with transcripts down-regulated (cluster 1, n=31) and up-regulated (cluster 2, n=15) in exposed gonads compared to controls (Supplementary file 3). Glutamine biosynthetic processes, positive regulation of insulin secretion, positive regulation of epithelial cell proliferation and ovarian follicle cell-cell adhesion were among the significantly enriched GO biological processes.

In oocytes, 81 transcripts were differentially expressed between the two treatments (p<0.01, FDR<5%, Supplementary file 5); 41 transcripts appeared to be down-regulated (cluster 1, n=41) and 40 up-regulated (cluster 2, n=40) in oocytes collected from exposed females compared with controls (Supplementary file 3). Proteolysis, embryo development and ion binding were some of the enriched GO biological processes. Finally, the proteome of oocytes revealed two abundant protein spots that showed a marked difference between exposed and control samples. These 2 spots were identified as arginine kinase, characterized by a lower amount in oocytes collected from exposed females and the protein severin, which was present in a higher amount in oocytes collected from exposed females than in oocytes collected from controls.

DEB model simulations

Control oysters were simulated with standard DEB-model parameters (action of energy used for growth plus somatic maintenance, Kappa = 0.45, and volume-specific cost of maintenance $[\dot{p}_M]$ = 44 J cm^{-3} day^{-1}) and with the absorption efficiency (AE) measured in the control (Figure 3, "control"). Exposed oysters were simulated with standard DEB model parameters and the absorption efficiency measured for this condition (Figure 3, "micro-PS.std"). Simulated relative differences in final dry flesh mass (DFM) and oocyte production were overestimated compared with values observed at T3. In order to make the model parameters fit with observed DFM and oocyte production, numerous simulations were performed with a set of parameter values (Kappa from 0 to 1 and $[\dot{p}_M]$ from 0 to 200 J cm^{-3} day^{-1}). The best fit between observations and simulations (Figure 3, "micro-PS.cal") was reached with a single set of the two parameters Kappa = 0.77 and $[\dot{p}_M]$ = 84 J cm^{-3} day^{-1}, which corresponds to increases of 71% and 90% beyond standard values, respectively.

Chemical analysis

Following methods described in Supplementary file 6, analyses on extracted micro-PS particles detected bibenzyl and 1(2H)naphtalenone,3,4,dihydro4phenyl with >90% correspondences (Supplementary file 6). Analyses in the aqueous phase or digestive styles did not show any molecules leaching from micro-PS particles compared with the controls, with a detection limit at 0.1 ng L^{-1} for compounds with a Log K_{ow} less than 3.

Discussion

Ingestion and fate of micro-PS in oyster

Micro-PS were efficiently ingested by filtration in oysters presumably due to their similarity in size and shape to phytoplankton. Oysters preferentially ingested the 6-µm micro-PS over the 2-µm diameter particles. This may be explained by the oyster particle selection mechanism, which is 100% efficient for 5 to 6-µm particles [27]. Ingested micro-PS particles were visually observed in feces (under microscope) and no accumulation in the gut was observed on histological slides, suggesting a high potential of egestion of micro-PS. However, smooth and spherical micro-PS beads differ greatly from plastic debris such as the fibers and fragments of varying form and roughness present in the marine environment. Therefore caution must be taken when extrapolating the rapid egestion rate observed here [28]. Despite evidence of MP translocation in bivalves from some other studies [14, 15, 17], here no evidence of micro-PS transfer from the digestive tract to the circulatory system and other tissues was detected on the histological slides. Future studies on marine bivalves should address translocation processes by testing non-spherical fragments down to nano-sized particles, the size class most prone to this phenomenon via transcellular uptake in the gastrointestinal epithelium in mammals [29].

Impacts of micro-PS on energy uptake and allocation

Consumption of microalgae and absorption efficiency appeared significantly higher in exposed oysters, suggesting a compensatory effect on food intake and absorption efficiency and an enhancement of mechanical digestion. Indeed, an improvement of mechanical disruption in the stomach of mussels was demonstrated in response to moderate silt ingestion, which enhances clearance rate and absorption efficiency [30]. Nevertheless, increased food consumption can be viewed as compensation to adjust energy intake in response to digestive interference caused by micro-PS in the gut. The variations in mRNA levels of lipid-related proteins such as enzymes involved in fatty acid oxidation also suggest impairment of fatty acid metabolism and reduced energy intake from food [31]. In any case, this compensation is insufficient to counterbalance the energy-flow disruption induced by micro-PS uptake as demonstrated by DEB modeling. Energy flows seem to shift toward organism maintenance and structural growth at the expense of reproduction. A recent study on mussels revealed increased energy consumption measured by respiration in MP-exposed animals,

suggesting increased stress and energy demand to maintain homeostasis [16]. Furthermore, in our data, there are signs of disturbance of homeostasis reflected by changes in hemocyte size and oxidative activity [32] and enrichment of transcripts involved in the response to glucocorticoid stimulus GO process. Glucocorticoids are hormonal corticosteroids involved in stress response, able to inhibit the expression of enzymes involved in fatty acid oxidation [33, 34].

Micro-PS impaired gametogenesis, gamete quality and fecundity

Strong negative effects were observed on reproductive health indices, which significantly impacted fecundity and offspring performance during larval stages. The 23% reduction in sperm velocity in exposed oysters may lower their ability to fertilize oocytes. Indeed, in sea urchin, a decrease in sperm motility was linked to an increase in the number of sperm required for fertilization success [35]. Oyster oocyte number and size in micro-PS exposed oysters were also significantly reduced over the same period (-38% and -5%, respectively). As oocyte quality predictors, mean oocyte diameter has been identified as a direct consequence of nutrition [36], supporting the hypothesis of energetic disruption in exposed oysters. Moreover, egg size and shape have been found to be positively related to larval survival and growth in subsequent progeny [37]. In oocytes, maternally inherited mRNAs can have multiple functions, from regulation of cell cycle progression and cellular metabolism, to regulation of developmental processes such as fertilization, activation of zygotic transcription, and formation of body axes [38]. Ion binding was greatly affected by MP exposure: 10 transcripts coding for proteins involved in this function were differentially expressed. Transcripts coding for proteins involved in Ca^{2+} binding may have affected the Ca^{2+} signaling pathway in exposed oocytes, thus affecting oocyte maturation [39]. Severin is a Ca^{2+}-dependent actin-binding protein regulating the completion of cell division [40]; its up-regulation may reflect a deleterious effect of micro-PS on cytoskeletal dynamics, which are essential during oocyte maturation, fertilization and subsequent embryo development [41]. Other candidates, down-regulated in exposed oocytes, also indicate potential impairment of embryo development: transcripts in the categories of embryogenesis, cell differentiation and proliferation, and the arginine kinase protein, responsible in invertebrates for ATP buffering on phosphagens, which are essential for embryo biosynthetic activities [42]. A large alteration in fecundity, estimated through D-larval yield, offspring growth and settlement, was observed for larvae produced from gametes collected from micro-PS exposed oysters. Negative effects of MP had already been observed on

fecundity in copepods using similar micro-PS [20], and in *Daphnia* exposed to nano-PS, where numbers and body size of neonates fell and malformation rates rose [21]. The parental effect of micro-PS on subsequent offspring growth may potentially affect recruitment of wild and farmed populations of Pacific oysters, with consequences for both ecology and aquaculture.

DEB modeling showed that the energy fraction allocated to reproduction seemed to shift towards structural growth and high maintenance costs. Disruption of energy balance may result from the down-regulation of several transcripts coding for proteins involved in the insulin pathway, with GO terms corresponding to cell proliferation and differentiation processes, in both digestive gland and gonads. The insulin pathway plays a crucial role in mobilizing reserves during gametogenesis, and has an essential role in germinal cell proliferation and maturation [43]. We thus hypothesize that micro-PS exposure negatively impacts cell proliferation and differentiation processes in gonads through the down regulation of genes responding to insulin signaling. Furthermore, a G-protein coupled receptor transcript, also down-regulated in digestive gland, has a key role in the reproductive function, binding the kisspeptin hormone, responsible for the gonadotropic axis in vertebrates [44]. The differential expression of hormone receptors or transcripts involved in different hormonal pathways in micro-PS exposed animals suggests endocrine disruption. Endocrine system function can be affected by factors such as stress or endocrine-disrupting chemicals. A disturbance in individual energetics revealed by DEB modeling suggested that micro-PS particles have threatened the physiological integrity of oysters and consequently increased the maintenance costs, as described in response to various stresses and species [45–47]. Micro-PS particles may potentially act as endocrine disruptors. The chemical analyses of virgin micro-PS only revealed bibenzyl and 1(2H)naphtalenone,3,4,dihydro4phenyl in destructive conditions after dichloromethane extraction. Bibenzyl-diol core molecules may have endocrine disruption properties, as established in mammal cells, because they are structural analogs of estrogens [48]. No substances were found in seawater or in the digestive style extracts used to mimic oyster digestive conditions *in vitro*. However, it is now known that endocrine disrupters are often present below the detection limits and that bio-assays are sometimes more powerful than chemical quantification methods to detect their presence and effect [49]. Although we cannot establish an impact of these molecules in our experiment, reprotoxic effects induced by virgin MP have recently been revealed in *Daphnia* [21] and in fish [50], suggesting that they could be a concern for endocrine disruption, induced by MP alone or in combination with other persistent pollutants.

7

Implications

The micro-PS concentration tested in the present study was below the one estimated in Besseling et al. [21] that may occur at the sediment−water interface, where wild oysters live (Supplementary File 7). The exposed mass concentration (0.023 mg L^{-1}) was also in the range of the highest estimated field concentration >333 μm, from manta trawl sampling (Supplementary File 7), based on the assumption of a steady fragmentation of plastic debris [9, 51]. It should, nonetheless, be noted that there is a lack of consistent field evaluations of the presence of microplastics as small as those used in the present study. This is mainly because of methodological limitations: current methods exclude the possibility of quantifying small size domains (reviewed by Filella [51]). Moreover, assuming no waste management infrastructure improvements, the cumulative quantity of plastic waste available to enter the marine environment from land is predicted to increase by an order of magnitude by 2025 [2], especially in estuaries and coastal waters where oysters live and where waters are greatly influenced by increased human expansion. Therefore, our study also contributes to an early warning system and provides stakeholders with the necessary data to limit the impact of the microplastic legacy in decades to come.

To conclude, this study highlighted microplastic impacts on energy uptake and allocation and on reproductive health indices (*i.e.* quantity and quality of gametes produced), when oysters were exposed to micro-PS during gametogenesis. Strong negative effects were shown on broodstock fecundity and offspring growth at larval stages. The two explanatory hypotheses discussed in the present paper, a fall in energy allocated to reproduction via interference in digestive processes and endocrine disruption, are not mutually exclusive. We believe that, considering the strength of the impact on reproductive health indices, both forms of disruption may have occurred. However, the absence of endocrine disruptor detection in biological samples prevents us from drawing stronger conclusions about this second hypothesis. Transcriptomic profiles support this hypothesis, notably highlighting an alteration in glucocorticoid response, insulin pathway and fatty-acid metabolism in oysters in response to micro-PS exposition. Further investigations are now necessary; first, to provide full environmental data on small microplastics <10 μm, requiring fundamental analytical developments ([51]) and, second, to compare our experimental results with *in situ* and/or experimental studies that

closely mimic *in situ* conditions, in particular by using different shapes and forms of MP representative of those found in the field.

Methods

Experimental exposure of adult oysters to micro-PS

The experimental procedures comply with French law and with institutional guidelines. Adult oysters purchased from a commercial hatchery (18 months, 16.9±5.3 g) were transferred to Ifremer's experimental facilities in March 2013. Histological visual inspection showed they were at reproductive stage 0 to early stage 1, corresponding to an undifferentiated state or developing early active gametogenesis [52]. After acclimatization, the oysters were conditioned for 2 months under suitable conditions for germ cell maturation [52]. They were placed in 6 experimental 50-L tanks (40 oysters *per* tank) supplied with filtered (1 μm), UV-treated running seawater (12.5 L h^{-1}) at 17.1 ± 0.5°C and 34 PSU, and fed continuously on a mixed diet of two microalgae (*Tisochrysis lutea,* formerly *Isochrysis* sp., Tahitian strain: T. iso; CCAP 927/14, and *Chaetoceros gracilis*, UTEX LB2658) at a daily ratio equal to 8% dry weight algae/dry weight oyster. Control and micro-PS exposed treatments were set up with 3 tanks *per* condition. For each treatment, a fourth tank was deployed without oysters to evaluate algal and micro-PS sinking or sticking to the tank walls. To prevent micro-PS sinking, the water inflow was pressurized to create recirculating flow in the tank, and air bubbling was used. To reduce MP clumping and sticking to the flask walls, micro-PS particles were supplied to tanks with Tween-20 at a final concentration of 0.0002%. The same concentration of Tween-20 was supplied to the control tanks.

The purchased micro-PS were yellow-green fluorescent polystyrene beads (2 and 6 μm, Polysciences, Inc). These were supplied continuously to the tanks by peristaltic pumps from a concentrated micro-PS solution, maintained in a glass flask on a magnetic stirrer. Micro-PS concentrations were daily counted on an EasyCyte Plus flow cytometer (Guava-Merck-Millipore, Darmstadt, Germany) giving an inflow concentration of 2,062±170 and 118±15 beads mL^{-1} for 2 and 6 μm particles, respectively (namely a mass concentration of 0.023 mg L^{-1}) corresponding to an inflow daily ratio of 9.6 mg micro-PS day^{-1}. The mass concentration in the surrounding water was of 0.01 mg L^{-1} (*i.e.* 1,816±76 and 21±6 beads mL^{-1} for 2 and 6 μm particles, respectively), which is far lower than most to which marine

9

invertebrates have been exposed (from 0.8 to 2500 mg L^{-1}) [10, 15, 17, 21] (Supplementary File 7). Microplastic concentration corresponded to 0.21% of the volume (µm^3) of algae supplied.

Ecophysiological measurements

Once a day, inflow and outflow seawater was sampled from each tank. Phytoplankton counts were made using an electronic particle counter (Multisizer 3 equipped with a 100-µm aperture tube) to provide 50 days of continuous data. Algal consumption (C) was expressed in algal cell volume *per* oyster *per* day (µm^3 oyster^{-1} d^{-1}), as in Savina and Pouvreau [53]. Polystyrene particle ingestion (I) was estimated in percentage micro-PS ingested: I=[(Ii-Io-Ib) / Ii] × 100, Ii being number of beads at the inlet, Io number of beads at the outlet, Ib number of beads remaining in the tank without oysters by subtracting inlet from outlet. Once a week, feces were collected from each tank to calculate the absorption efficiency (AE, %) of organic matter from ingested food [53].

Sampling

At the beginning and the end of the experiment, 12 oysters *per* condition were sacrificed to measure biometric parameters (total, shell and dry weight). Condition index (CI) was calculated as: dry weight / (total weight-shell weight). At 2, 5 and 8 weeks after the beginning of exposure (corresponding to T1, T2 and T3, respectively), 8 animals *per* tank were sampled for flesh weight, hemolymph (taken as described by Haberkorn et al. [54]), and a transversal section of the gonadic area for histological examination. The remainder of the gonad and digestive gland were immediately frozen in liquid nitrogen for subsequent analyses. Oocytes were collected from 5 females *per* treatment, filtered in a 40-µm sieve, counted and transferred into 1.5 mL Extract-all reagent (Eurobio, Courtaboeuf, France) (20,000 oocytes) and 5 mL lysis buffer [55] (200,000 oocytes) for RNA and protein analyses, respectively. For gamete quality measurements and larval rearing, gametes were collected at T3 in 9 control and 9 exposed animals of each sex by stripping the gonads.

Gamete quality analyses

Sperm movement was triggered using a two-step dilution in an activating solution and analyzed using a CASA plug-in for Image J software. The percentage of motile spermatozoa and their velocity (VAP: Velocity of the Average Path) were assessed on a minimum of 30 spermatozoa, according to Suquet

et al. [56]. Oocyte diameter was assessed using Image J, by measuring Feret diameter. Triplicate lots of 25,000 oocytes *per* exposed and control female were fertilized using a non-limiting sperm to oocyte ratio from a pool of 3 control males. D-larval yield was estimated at 48 h post fertilization: (number of D-larvae/25,000 eggs)*100.

Larval rearing

To test for impact on offspring, fertilizations were performed in triplicate for each condition, 3 pools of oocytes were fertilized separately using a pool of sperm at a ratio of 30 spermatozoa/oocyte. Embryos were maintained 48 h at 25°C in 150-L tanks in 1-µm filtered seawater at a concentration of 50 embryo mL^{-1}. D-larvae were then transferred to 5-L cylindrical triplicate tanks at the density of 50 larvae mL^{-1}, and maintained in a flow-through rearing system (50% seawater renewal h^{-1}, 25°C, 34 PSU). Algae (*T. lutea* and *C. gracilis*) were continuously supplied as described by Gonzales-Araya et al. [57]. Larvae were sampled every 2-3 days and stored in a 0.1% formaldehyde-seawater solution until image analysis for size monitoring. Morphological competence for metamorphosis was determined when ≥50% of larvae reached the eyed-larvae stage. Larval size was assessed by measuring shell length using image analysis on at least 30 larvae *per* tank *per* day of sampling (WinImager 2.0 and Imaq Vision Builder 6.0 software for image capture and analysis, respectively).

Hemolymph flow cytometry analysis

Morphological parameters and oxidative activity of hemocyte sub-populations were measured as described by Haberkorn et al. [54] on 50 µL hemolymph using a FACScalibur (BD Biosciences, San Jose, CA, USA) flow cytometer (FCM), equipped with a 488-nm argon laser.

Histology

A 3-mm cross section of the visceral mass was excised in front of the pericardic region and immediately fixed in modified Davidson's solution [52], n-butyl alcohol was used as a fixative to preserve the fluorescent polystyrene beads [58]. Slides were examined under a light microscope to determine gametogenic stage. Presence of micro-PS in tissues was determined by examination of histological slides under a LEICA DMIRB inverted microscope (Leica Microsystems Inc.111 Deerlake

Road Deerfield, IL 60015). Pictures were taken using a Retigua 2000R color camera and ImageJPro software.

Protein extraction and proteomic analysis

Total proteins were extracted and analyzed using two-dimensional electrophoresis, spots were quantified in Coomassie-blue stained gels as in Corporeau et al. [55]. In-gel digestion was performed for excised spots based on their differential expression, as quantified using Progenesis[TM] SameSpots v1.5 software (Nonlinear Dynamics, Newcastle upon Tyne, UK), followed by LC-MS/MS analyses [55].

RNA extraction, amplification, labeling and microarray hybridization

Total RNA was isolated using Extract-all reagent (Eurobio) at a concentration of 1 ml/50 mg powder, treated with DNAse I (Sigma, 1U μg^{-1} total RNA) and assayed for concentration and quality following Sussarellu et al. [59]. For microarray hybridizations, 200 ng of total RNA (51 samples for gonads and digestive gland from females sampled at T1 and T3; and 8 oocyte samples taken at T3) were indirectly labeled with Cy3, using the Low Input Quick Amp labeling kit. Hybridization and scanning were performed on Agilent 60-mer 4x44K custom microarrays containing 31,918 *C. gigas* contigs [59].

Preprocessing and microarray data analysis

Microarray data were processed and analyzed using the language R/BioConductor [60] as in Sussarellu et al. [59]. Normalized hybridization values were deposited in the gene expression omnibus (GEO) repository with the accession number GSE71845. Statistical analyses to identify the differentially expressed transcripts in digestive glands and gonads were carried out by ANOVA. The fixed factors for the two-way ANOVA were treatment (MP exposure *vs* control) and sampling time (T1 or T3). For oocytes, differentially expressed transcripts were detected by t-test. The false discovery rate (FDR) associated with the selected transcripts was determined by: [total number of analyzed transcripts (31,918)×*p*-value/number of differentially expressed transcripts]×100; the FDR cut-off value was 5%. Hierarchical clustering was performed using the Ward method, and 1-correlation as dissimilarity matrix. Putative annotations of transcripts were identified using ngKlast software (KL Korilog Bioinformatics Solutions) against a protein database (E-value $1.0×10e^{-5}$) obtained from the *C. gigas* sequenced genome and transcriptome on Genbank [61]. GO terms were obtained using

ngKlast against the Swissprot database (E-value $1.0 \times 10e^{-5}$). GO terms enrichment analysis was performed using the Fisher's Exact test on Blast2Go [62].

Dynamic Energy Budget Design

The Dynamic Energy Budget (DEB) model simulations were performed as in Bernard et al. [63] to evaluate how physiological changes induced by micro-PS exposition affect energy fluxes and could explain observed phenotypic changes. The DEB model describes dynamics of four state variables: (1) the energy stored in reserves, E; (2) energy allocated to structural growth, E_V; (3) energy allocated to development and reproduction, E_R; and (4) energy used in the construction of gametes, E_{GO} (see [63] for a full description). Initial state was obtained from the initial biometrics measurements and maturity observations. Oocyte production was calculated according to an energy content of 9.3×10^{-4} J oocyte^{-1}. Two parameters, namely the allocation fraction to structural growth and structural maintenance from reserves (the remainder being allocated to development/reproduction and maturity maintenance, Kappa) and the volume specific cost for maintenance rate ($[\dot{p}_M]$, J cm^{-3} day^{-1}), were free fitted in order to evaluate the disturbance level in terms of micro-PS exposure that would lead to the observed growth and reproductive traits.

Statistical Analysis

All analysis data were processed and analyzed using the language R/BioConductor [60], R Development Core Team 2008) by ANOVA (fixed factors were condition and sampling date) or t-tests. Normality was screened on residuals and further tested using the Shapiro-Wilk test. When necessary, data were log transformed, and angular transformation was used for percentage data. Homogeneity of variance matrices was assessed with a Fligner test. Least significant difference post-hoc tests (LSD test) were performed in order to discriminate groups. Data are expressed as mean ± confidence intervals (α=5%). Analyses of microarray data are detailed above in the microarray data analysis section.

Acknowledgements

References

1. Rochman CM, Browne MA, Halpern BS, et al. (2013) Policy: Classify plastic waste as hazardous. *Nature* 494:169–171.

2. Jambeck JR, Geyer R, Wilcox C, et al. (2015) Plastic waste inputs from land into the ocean. *Science (80-)* 347:768–771.

3. Wilcox C, Van Sebille E, Hardesty BD (2015) Threat of plastic pollution to seabirds is global, pervasive, and increasing. Proc Natl Acad Sci U S A. doi: 10.1073/pnas.1502108112

4. Arthur C, Baker J, Bamford H (2009) Proceedings of the International Research Workshop on the Occurrence, Effects, and Fate of Microplastic Marine Debris. In: NOAA Tech. Memo. NOS-OR&R-30. p 530

5. Costa MF, Ivar do Sul JA, Silva-Cavalcanti JS, et al. (2010) On the importance of size of plastic fragments and pellets on the strandline: a snapshot of a Brazilian beach. *Environ Monit Assess* 168:299–304.

6. Andrady AL (2011) Microplastics in the marine environment. *Mar Pollut Bull* 62:1596–1605.

7. Cole M, Lindeque P, Halsband C, Galloway TS (2011) Microplastics as contaminants in the marine environment: A review. *Mar Pollut Bull* 62:2588–2597.

8. Eriksen M, Lebreton LCM, Carson HS, et al. (2014) Plastic Pollution in the World's Oceans: More than 5 Trillion Plastic Pieces Weighing over 250,000 Tons Afloat at Sea. *PLoS One* 9:e111913.

9. Cozar A, Echevarria F, Gonzalez-Gordillo JI, et al. (2014) Plastic debris in the open ocean. *Proc Natl Acad Sci U S A* 111:10239–10244.

10. Wegner A, Besseling E, Foekema E m., et al. (2012) Effects of nanopolystyrene on the feeding behavior of the blue mussel (*Mytilus edulis* L.). *Environ Toxicol Chem* 31:2490–2497.

11. Cole M, Lindeque P, Fileman E, et al. (2013) Microplastic Ingestion by Zooplankton. *Environ Sci Technol* 47:6646–6655.

12. Browne MA, Niven SJ, Galloway TS, et al. (2013) Microplastic moves pollutants and additives to worms, reducing functions linked to health and biodiversity. *Curr Biol* 23:2388–2392.

13. Wright SL, Rowe D, Thompson RC, Galloway TS (2013) Microplastic ingestion decreases energy reserves in marine worms. *Curr Biol* 23:R1031–R1033.

14. Browne MA, Dissanayake A, Galloway TS, et al. (2008) Ingested Microscopic Plastic Translocates to the Circulatory System of the Mussel, *Mytilus edulis* (L.). *Environ Sci Technol* 42:5026–5031.

15. Von Moos N, Burkhardt-Holm P, Köhler A (2012) Uptake and Effects of Microplastics on Cells and Tissue of the Blue *Mussel Mytilus* edulis L. after an Experimental Exposure. *Environ Sci Technol* 46:11327–11335.

16. Cauwenberghe L Van, Claessens M, Vandegehuchte MB, Janssen CR (2015) Microplastics are taken up by mussels (*Mytilus edulis*) and lugworms (*Arenicola marina*) living in natural habitats. *Environ Pollut* 199:10–17.

17. Avio CG, Gorbi S, Milan M, et al. (2015) Pollutants bioavailability and toxicological risk from microplastics to marine mussels. *Environ Pollut* 198C:211–222.

18. Graham ER, Thompson JT (2009) Deposit- and suspension-feeding sea cucumbers (Echinodermata) ingest plastic fragments. *J Exp Mar Bio Ecol* 368:22–29.

19. Besseling E, Wegner A (2012) Effects of microplastic on fitness and PCB bioaccumulation by the lugworm *Arenicola marina* (L.). *Environ Sci Technol* 47:593–600.

20. Lee K-WW, Shim WJ, Kwon OY, Kang J-HH (2013) Size-dependent effects of micro polystyrene particles in the marine copepod tigriopus japonicus. *Environ Sci Technol* 47:11278–11283.

21. Besseling E, Wang B, Lu M, et al. (2014) Nanoplastic Affects Growth of *S. obliquus* and Reproduction of *D. magna*. *Environ Sci Technol* 48:12336–12343.

22. Cole M, Lindeque P, Fileman E, et al. (2015) The impact of polystyrene microplastics on feeding, function and fecundity in the marine copepod *Calanus helgolandicus*. *Environ Sci Technol* 49:1130–7.

23. Teuten EL, Rowland SJ, Galloway TS, Thompson RC (2007) Potential for Plastics to Transport Hydrophobic Contaminants. *Environ Sci Technol* 41:7759–7764.

24. Chapman RW, Mancia A, Beal M, et al. (2011) The transcriptomic responses of the eastern oyster, *Crassostrea virginica*, to environmental conditions. *Mol Ecol* 20:1431–1449.

25. Barnes DK a, Galgani F, Thompson RC, Barlaz M (2009) Accumulation and fragmentation of plastic debris in global environments. *Philos Trans R Soc B Biol Sci* 364:1985–1998.

26. Browne MA, Galloway TS, Thompson RC (2010) Spatial Patterns of Plastic Debris along Estuarine Shorelines. *Environ Sci Technol* 44:3404–3409.

27. Ward JE, Shumway SE (2004) Separating the grain from the chaff: particle selection in suspension- and deposit-feeding bivalves. *J Exp Mar Bio Ecol* 300:83–130.

28. Lusher a. L, McHugh M, Thompson RC (2013) Occurrence of microplastics in the gastrointestinal tract of pelagic and demersal fish from the English Channel. *Mar Pollut Bull* 67:94–99.

29. Hussain N (2001) Recent advances in the understanding of uptake of microparticulates across the gastrointestinal lymphatics. *Adv Drug Deliv Rev* 50:107–142.

30. Navarro E, Iglesias JIPIP, Camacho APP, Labarta U (1996) The effect of diets of phytoplankton and suspended bottom material on feeding and absorption of raft mussels (*Mytilus galloprovincialis* Lmk). *J Exp Mar Bio Ecol* 198:175–189.

31. Bayne BL (2004) Phenotypic flexibility and physiological tradeoffs in the feeding and growth of marine bivalve molluscs. *Integr Comp Biol* 44:425–432.

32. Donaghy L, Kraffe E, Le Goïc N, et al. (2012) Reactive Oxygen Species in Unstimulated Hemocytes of the Pacific Oyster *Crassostrea gigas*: A Mitochondrial Involvement. PLoS One. doi: 10.1371/journal.pone.0046594

33. Nagao M, Parimoo B, Tanaka K (1993) Developmental, nutritional, and hormonal regulation of tissue-specific expression of the genes encoding various acyl-CoA dehydrogenases and alpha-subunit of electron transfer flavoprotein in rat. *J Biol Chem* 268:24114–24124.

34. Letteron P, Brahimi-Bourouina N, Robin MA, et al. (1997) Glucocorticoids inhibit mitochondrial matrix acyl-CoA dehydrogenases and fatty acid beta-oxidation. *Am J Physiol Gastrointest Liver Physiol* 272:G1141–1150.

35. Levitan DR (2000) Sperm velocity and longevity trade off each other and influence fertilization in the sea urchin *Lytechinus variegatus*. *Proc Biol Sci* 267:531–4.

36. Cannuel R, Beninger PG (2005) Is oyster broodstock feeding always necessary? A study using oocyte quality predictors and validators in *Crassostrea gigas*. *Aquat Living Resour* 18:35–43.

37. Baynes SM, Howell BR (1996) The influence of egg size and incubation temperature on the condition of *Solea solea* (L.) larvae at hatching and first feeding. *J Exp Mar Bio Ecol* 199:59–77.

38. Mtango NR, Potireddy S, Latham KE (2008) Oocyte quality and maternal control of development. *Int Rev Cell Mol Biol* 268:223–90.

39. Leclerc C, Guerrier P, Moreau M (2000) Role of dihydropyridine-sensitive calcium channels in meiosis and fertilization in the bivalve molluscs *Ruditapes philippinarum* and *Crassostrea gigas*. *Biol Cell* 92:285–299.

40. Rohlfs M, Arasada R, Batsios P, et al. (2007) The Ste20-like kinase SvkA of *Dictyostelium discoideum* is essential for late stages of cytokinesis. *J Cell Sci* 120:4345–54.

41. Sinsimer KS, Lee JJ, Thiberge SY, Gavis ER (2013) Germ plasm anchoring is a dynamic state that requires persistent trafficking. *Cell Rep* 5:1169–77.

42. Iyengar MR, Iyengar CWL, Chen HY, et al. (1983) Expression of creatine kinase isoenzyme during oogenesis and embryogenesis in the mouse. *Dev Biol* 96:263–268.

43. Gricourt L, Mathieu M, Kellner K (2006) An insulin-like system involved in the control of Pacific oyster *Crassostrea gigas* reproduction: hrIGF-1 effect on germinal cell proliferation and maturation associated with expression of an homologous insulin receptor-related receptor. *Aquaculture* 251:85–98.

44. Tena-Sempere M (2006) The roles of kisspeptins and G protein-coupled receptor-54 in pubertal development. *Curr Opin Pediatr* 18:442–7.

45. Kooijman SALM (2010) Dynamic Energy Budget Theory for Metabolic Organisation. Cambridge University Press

46. Muller EB, Nisbet RM, Berkley HA (2010) Sublethal toxicant effects with dynamic energy budget theory: model formulation. *Ecotoxicology* 19:48–60.

47. Huvet A, Béguel J-P, Cavaleiro NP, et al. (2015) Disruption of amylase genes by RNA interference affects reproduction in the Pacific oyster *Crassostrea gigas*. *J Exp Biol* 218:1740–1747.

48. Waibel M, De Angelis M, Stossi F, et al. (2009) Bibenzyl- and stilbene-core compounds with non-polar linker atom substituents as selective ligands for estrogen receptor beta. *Eur J Med Chem* 44:3412–24.

49. Kiyama R, Wada-Kiyama Y (2015) Estrogenic endocrine disruptors: Molecular mechanisms of action. *Environ Int* 83:11–40.

50. Rochman CM, Kurobe T, Flores I, Teh SJ (2014) Early warning signs of endocrine disruption in adult fish from the ingestion of polyethylene with and without sorbed chemical pollutants from the marine environment. *Sci Total Environ* 493:656–661.

51. Filella M (2015) Questions of size and numbers in environmental research on microplastics: methodological and conceptual aspects. *Environ Chem* 12:527.

52. Fabioux C, Huvet A, Le Souchu P, et al. (2005) Temperature and photoperiod drive *Crassostrea gigas* reproductive internal clock. *Aquaculture* 250:458–470.

53. Savina M, Pouvreau S (2004) A comparative ecophysiological study of two infaunal filter-feeding bivalves: and *Glycymeris glycymeris*. *Aquaculture* 239:289–306.

54. Haberkorn H, Lambert C, Le Goïc N, et al. (2014) Cellular and biochemical responses of the oyster *Crassostrea gigas* to controlled exposures to metals and *Alexandrium minutum*. *Aquat Toxicol* 147:158–67.

55. Corporeau C, Vanderplancke G, Boulais M, et al. (2012) Proteomic identification of quality factors for oocytes in the Pacific oyster *Crassostrea gigas*. *J Proteomics* 75:5554–5563.

56. Suquet M, Labbé C, Puyo S, et al. (2014) Survival, growth and reproduction of cryopreserved larvae from a marine invertebrate, the Pacific oyster (*Crassostrea gigas*). *PLoS One* 9:e93486.

57. Gonzalez Araya R, Mingant C, Petton B, Robert R (2012) Influence of diet assemblage on *Ostrea edulis* broodstock conditioning and subsequent larval development. *Aquaculture* 364-365:272–280.

58. Callebaut M, Meeussen C (1989) Method for the Preservation of Polystyrene Latex Beads in Tissue Sections. 2:100–102.

59. Sussarellu R, Huvet A, Lapègue S, et al. (2015) Additive transcriptomic variation associated with reproductive traits suggest local adaptation in a recently settled population of the Pacific oyster, Crassostrea gigas. *BMC Genomics* 16:808.

60. Gentry J, Hornik K, Hothorn T, et al. (2004) Bioconductor: open software development for computational biology and bioinformatics. *Genome Biol* 5:R80.

61. Zhang G, Fang X, Guo X, et al. (2012) The oyster genome reveals stress adaptation and complexity of shell formation. *Nature* 490:49–54.

62. Conesa A, Gotz S, Garcia-Gomez JM, et al. (2005) Blast2GO: a universal tool for annotation, visualization and analysis in functional genomics research. *Bioinformatics* 21:3674–3676.

63. Bernard I, de Kermoysan G, Pouvreau S (2011) Effect of phytoplankton and temperature on the reproduction of the Pacific oyster *Crassostrea gigas*: Investigation through DEB theory. *J Sea Res* 66:349–360.

64.   Lacroix C, Le Cuff N, Receveur J, et al. (2014) Development of an innovative and "green" stir bar sorptive extraction-thermal desorption-gas chromatography-tandem mass spectrometry method for quantification of polycyclic aromatic hydrocarbons in marine biota. *J Chromatogr A* 1349:1–10.

65.   Gilfillan LR, Ohman MD, Doyle MJ, Watson W (2009) Occurrence of plastic micro-debris in the southern california current system. *CalCOFI Rep* 50:123–133.

66.   Eriksen M, Maximenko N, Thiel M, et al. (2013) Plastic pollution in the South Pacific subtropical gyre. *Mar Pollut Bull* 68:71–76.

67.   Moore CJ, Moore SL, Leecaster MK, Weisberg SB (2001) A Comparison of Plastic and Plankton in the North Pacific Central Gyre. *Mar Pollut Bull* 42:1297–1300.

68.   Lechner A, Keckeis H, Lumesberger-Loisl F, et al. (2014) The Danube so colourful: A potpourri of plastic litter outnumbers fish larvae in Europe's second largest river. *Environ Pollut* 188:177–181.

69.   Reddy MS, Adimurthy S, Ramachandraiah G (2006) Description of the small plastics fragments in marine sediments along the Alang-Sosiya ship-breaking yard, India. *Estuar Coast Shelf Sci* 68:656–660.

70.   Claessens M, Meester S De, Landuyt L Van, et al. (2011) Occurrence and distribution of microplastics in marine sediments along the Belgian coast. *Mar Pollut Bull* 62:2199–2204.

Figure legends

Figure 1. Histology panels: Micro-polystyrene beads of 2 and 6 µm were observed in the stomach lumen (A and B) and intestine (C and D) of exposed oysters but not in the digestive tubules (E). No beads were observed in control oysters. ct: conjunctive tissue; ce: ciliated epithelium; cs: crystalline style; lu: lumen; dt: digestive tubule, 6 µm: 6-µm polystyrene beads, 2 µm: 2-µm polystyrene beads.

Figure 2. Larval growth: Larval size up to metamorphosis. Larval groups were obtained by crossing gametes collected from control genitors (control progeny) and from oysters exposed to micro-polystyrene beads (MP progeny). A settlement delay of 6 days was observed in MP progeny compared with controls. For each group, mean and confidence intervals were obtained from triplicate larval rearing (N>30).

Figure 3. DEB modeling: DEB model simulations for the dry flesh mass (DFM) and oocyte number. Simulations named "control" represent simulations with standard parameters (*i.e.* fraction of energy allocated to soma, Kappa = 0.45, and volume specific cost for maintenance, $[\ddot{p}_M]$ = 44 J cm^{-3} day^{-1}) and with absorption efficiency measured in controls. Simulations named "micro-PS.std" represent simulations with standard parameters and with absorption efficiency measured for oysters exposed to micro-polystyrene. Simulations named "micro-PS.cal" represent simulations with calibrated parameters (*i.e.* Kappa = 0.77 and $[\ddot{p}_M]$ = 84 J cm^{-3} day^{-1}) and with absorption efficiency measured for exposed oysters. Initial and final dry flesh mass and oocyte production observed are plotted.

Supplementary information

Supplementary file 1. Boxplots of oyster hemocyte parameters showing significant condition effect or condition-time interaction in the two-way ANOVA. T1 = sampling time 1 (2 weeks of micro-PS exposure), T2 = sampling time 2 (5 weeks), T3 = sampling time 3 (8 weeks); MP = micro-polystyrene exposed oysters, C = control oysters (N=24). Letters represent statistically different groups calculated by the LSD test.

Supplementary file 2. Differentially expressed transcripts in female oyster digestive glands between micro-PS and control treatments: Genbank accession, best hit, fold changes, heatmap clusters and GO enriched terms.

Supplementary file 3. Heatmaps of differentially expressed transcripts in female oyster digestive glands (A), gonads (B) and oocytes (C). For A and B, columns represent the averaged mRNA levels for each group (n=5–8; T1 = sampling time 1, 2 weeks of exposure; T3 = sampling time 3, 8 weeks of exposure; MP = oysters exposed to polystyrene microbeads, T = control oysters). For C, individual samples are presented corresponding to oocytes collected in 3 exposed and 5 control females. Expression levels are shown with a color scale in which shades of red represent higher expression and shades of green represent lower expression.

Supplementary file 4. Differentially expressed transcripts in female oyster gonads between micro-PS and control treatments: Genbank accession, best hit, fold changes, heatmap clusters and GO enriched terms.

Supplementary file 5. Differentially expressed transcripts in oocytes between micro-PS and control treatments: Genbank accession, best hit, fold changes, heatmap clusters and GO enriched terms.

Supplementary file 6. Micro-PS chemical analysis: Scan chromatogram of micro-PS extracted with dichloromethane (A). Superimposed scan chromatograms of control digestive styles (black) and digestive styles with micro-PS particles (red) (B).

Supplementary file 7. Highest microplastic concentrations measured in nature and used in some experimental studies, including the present one.

Figure 1
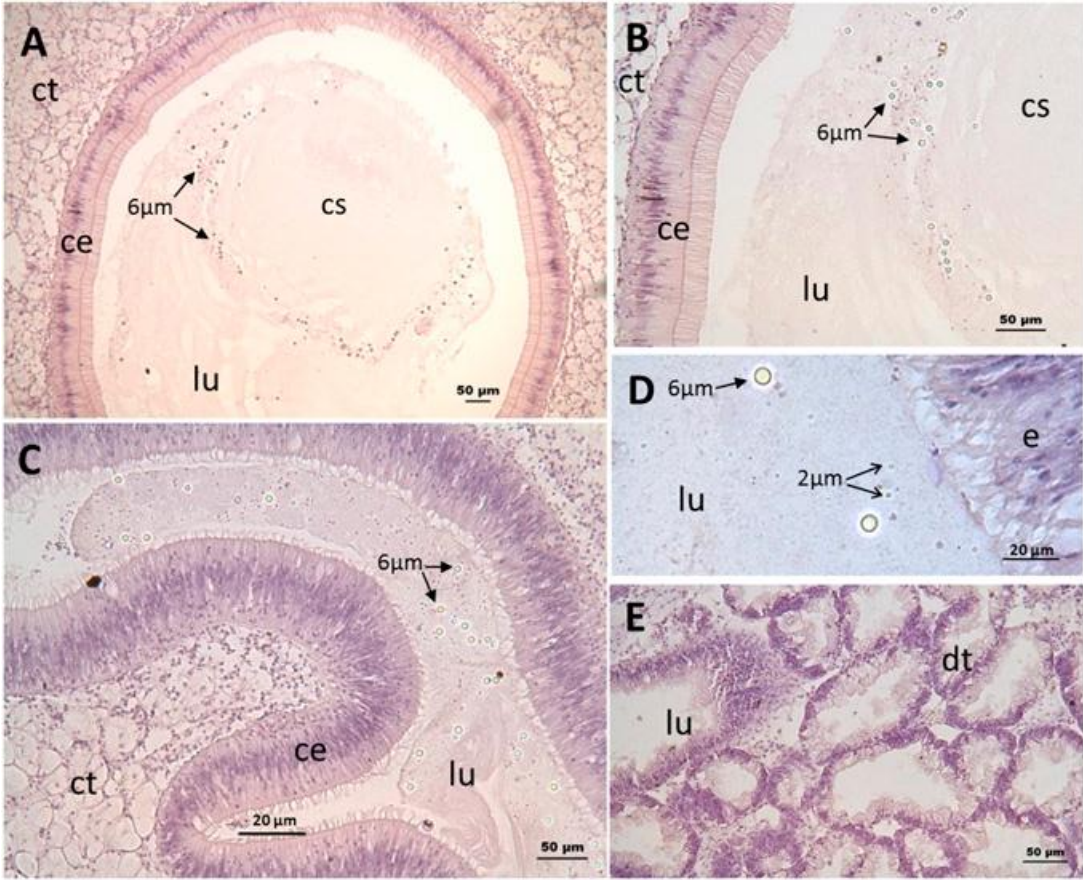
Figure 2
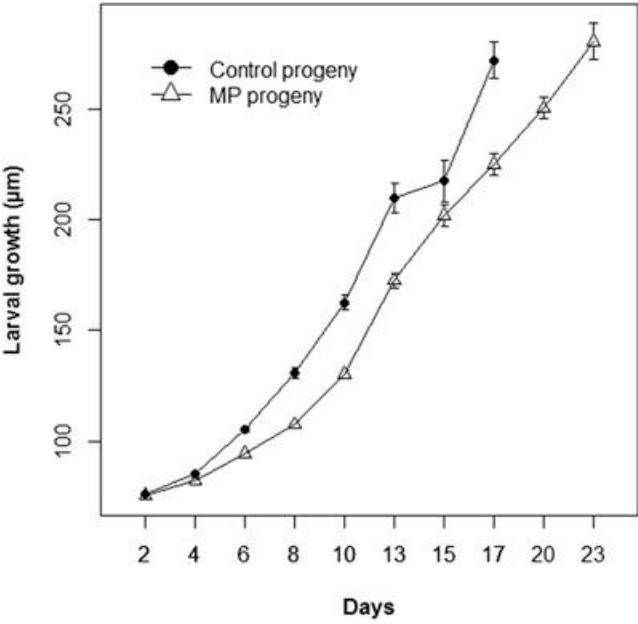
Figure 3
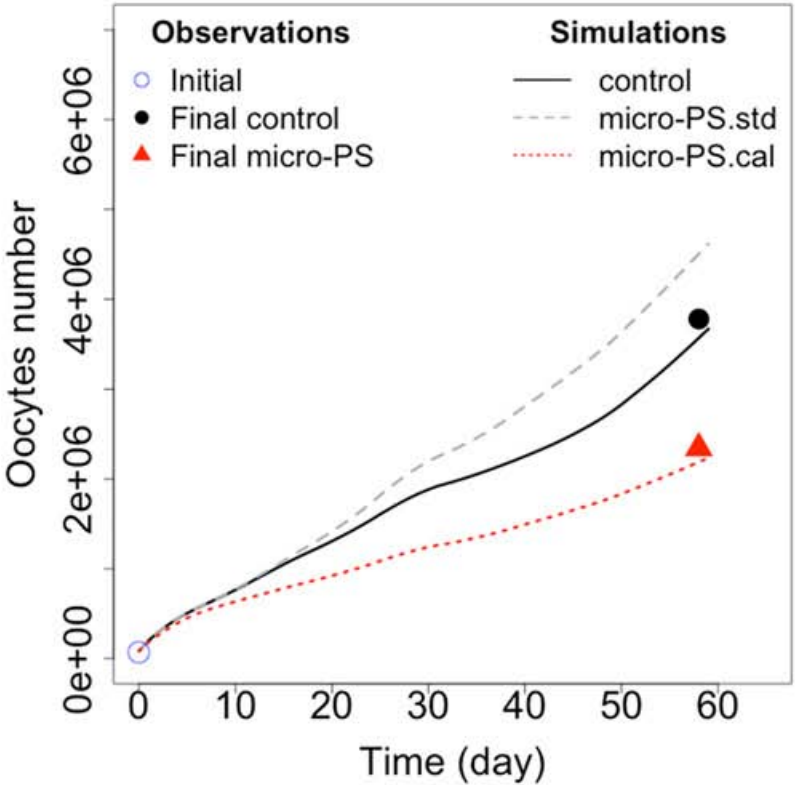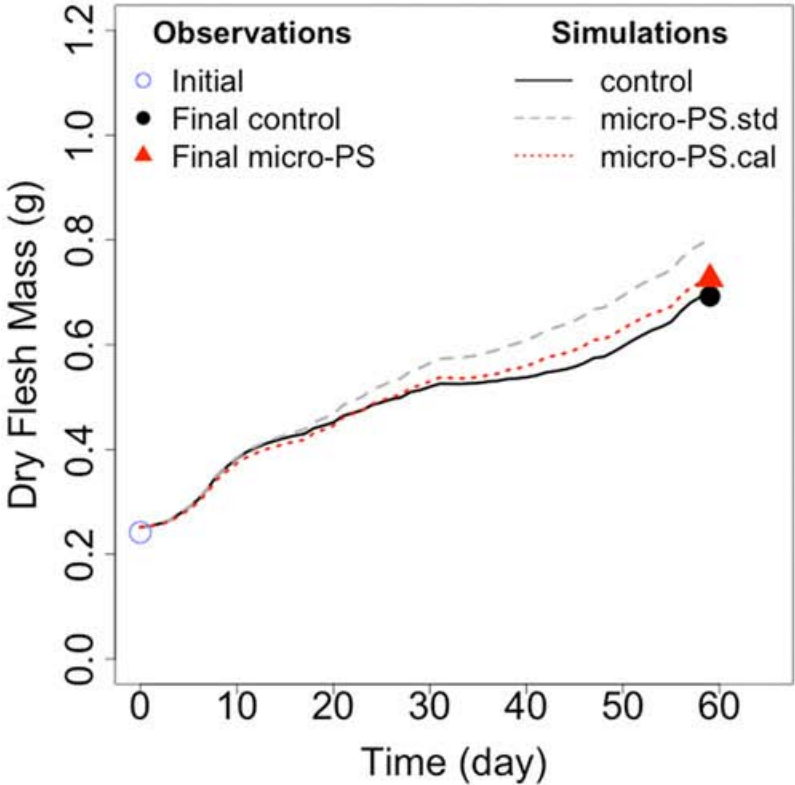
Figure S1
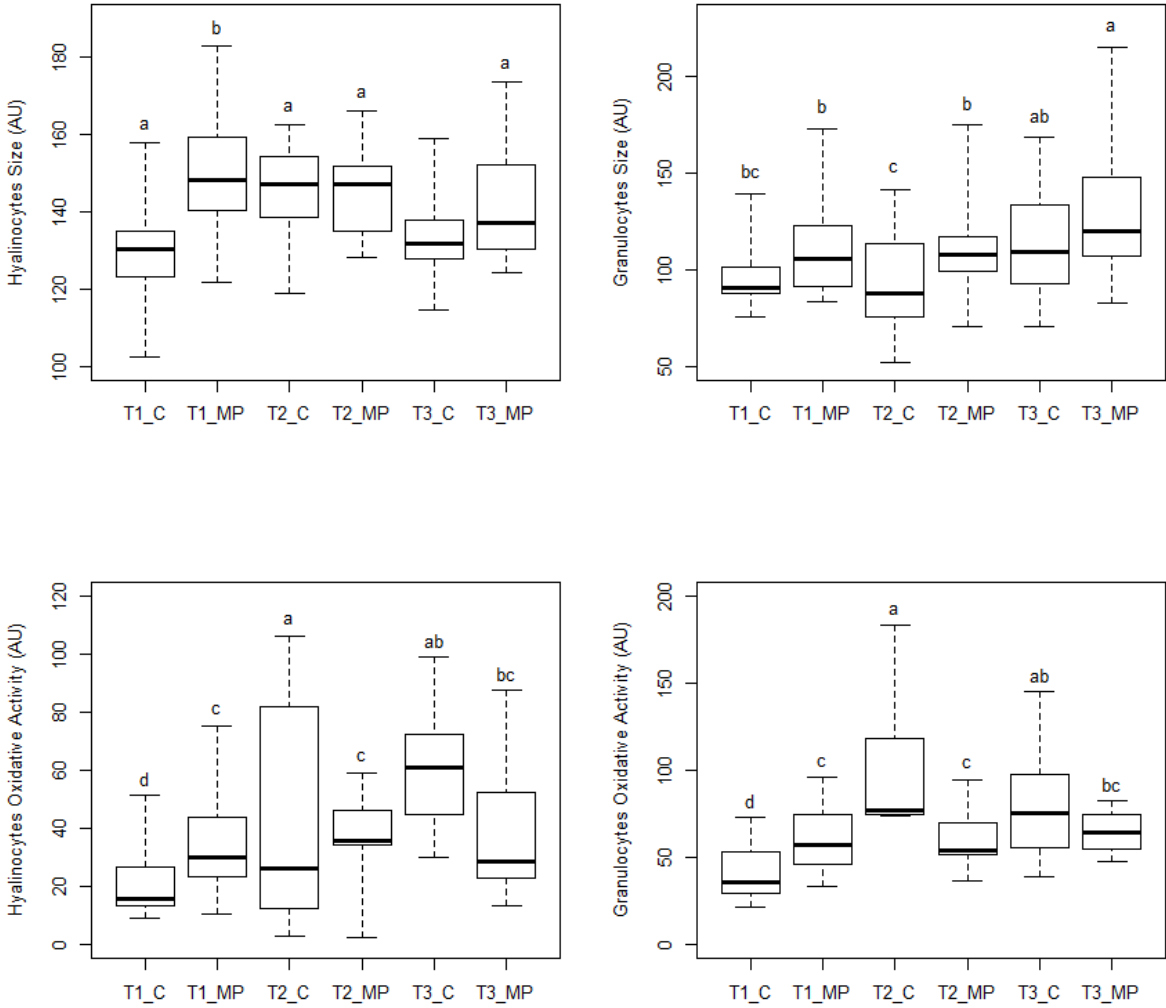
Cluster	GenBank	Hit_Definition	FoldChange
1	CU992177		0,96
1	CU989017	hypothetical protein CGI_10009186	0,97
1	CU992923	hypothetical protein CGI_10006558	0,70
1	CF369202		0,98
1	CU996638		0,98
1	AM855937		0,90
1	ES789647	hypothetical protein CGI_10016320	0,92
1	CU986563		0,95
1	CU987838		0,89
1	CU989662	hypothetical protein CGI_10023065	0,98
1	CU986646		0,93
1	AM860551		0,98
1	CU682913	Tripartite motif-containing protein 2	0,93
1	CU989075		0,97
1	BQ427136		0,98
1	AM858308	hypothetical protein CGI_10000712	0,92
1	CU988676	hypothetical protein CGI_10019000	0,92
1	EW777782		0,93
1	CU986781	Short-chain specific acyl-CoA dehydrogenase, mitochondrial	0,91
1	CU990320	hypothetical protein CGI_10004063	0,98
1	EE677605		0,98
1	EW777715		0,88
1	FP010002	Vacuolar protein sorting-associated protein VTA1-like protein	0,98
1	AM865430	hypothetical protein CGI_10016192	0,96
1	BQ426240		0,98
1	AM856457		0,96
1	FP003332	hypothetical protein CGI_10012708	0,92
1	AM863859		0,99
1	AM860922	Neural-cadherin	0,88
1	FP011719	Proline-rich transmembrane protein 1	0,87
1	BG467430	Sodium- and chloride-dependent glycine transporter 2	0,93
1	AM868898		0,95
1	CU685529		0,96
1	CU991544	Tudor domain-containing protein 12	0,92
1	AM858508	Parathyroid hormone/parathyroid hormone-related peptide recept	0,95
1	AM860917		0,85
1	CU986472	Peptidyl-prolyl cis-trans isomerase SDCCAG10	0,97
1	CU990629	G-protein coupled receptor 54	0,95
1	CU992489	Cytochrome b-245 light chain	0,90
1	AM860025	Uncharacterized protein C16orf48	0,91
1	CU997244	Cytoskeleton-associated protein 2	0,95
1	CU989792	Aquaporin-4	0,94
1	CU684258	Neurotrypsin	0,90
1	AM858491	Very long-chain specific acyl-CoA dehydrogenase, mitochondrial	0,91
1	CU994860	Sushi repeat-containing protein SRPX2	0,98
1	FP002803	Solute carrier family 2, facilitated glucose transporter member 8	0,97
1	CU991366	Pancreatic lipase-related protein 1	0,84
1	FP003376		0,93
1	FP010293	PR domain zinc finger protein 16	0,98
1	DV736323	hypothetical protein CGI_10012811	0,80

1	AM861879	von Willebrand factor D and EGF domain-containing protein	0,92
2	AM854579	hypothetical protein CGI_10020615	1,37
2	BQ426805	Tripartite motif-containing protein 2	1,03
2	AM856435	hypothetical protein CGI_10018346	1,05
2	CU995380	hypothetical protein CGI_10022503	1,09
2	AM861538	Dynein heavy chain 1, axonemal	1,06
2	CU996417		1,16
2	CU986763	hypothetical protein CGI_10017337	1,13
2	AM865796		1,18
2	AM868839	Interferon-induced protein 44-like protein	1,25
2	AM855324	Nephrin	1,07
2	AM867385		1,04
2	CU997769	hypothetical protein CGI_10020280	1,02
2	CU987657	hypothetical protein CGI_10008841	1,09
2	CU991705	TCF3 fusion partner-like protein	1,03
2	CU685707	Agrin	1,11
2	CU987595	Tropomyosin	1,05
2	CU683365		1,08
2	EW777630	Putative RNA exonuclease NEF-sp	1,07
2	AM866995	Phosphoglycerate kinase 1	1,08
2	AM853389	Lipoxygenase-like protein domain-containing protein 1	1,04
2	CU996322		1,06
2	AM868494	hypothetical protein CGI_10020493	1,09
2	AM861856	Transducin beta-like protein 2	1,05
2	CU989941	A-kinase anchor protein 14	1,06
2	CU996544	hypothetical protein CGI_10001188	1,05

Cluster	Genbank	Hit_Definition	Fold Change
1	CU997052	Proto-oncogene tyrosine-protein kise ROS	0,96
1	CU989931	60S ribosomal protein L4	0,97
1	FP005107	hypothetical protein CGI_10022173	0,95
1	CU984035	TraB domain-containing protein	0,97
1	CB617476		0,97
1	CU999681	Transcriptiol-regulating factor 1	0,95
1	CU682669	Cadherin-23	0,98
1	AM853762		0,97
1	ES789204		0,97
1	FP003706	28S ribosomal protein S16, mitochondrial	0,97
1	AM858544		0,94
1	CU988664	hypothetical protein CGI_10007113	0,96
1	CU988329	Beta-1,3-galactosyltransferase 1	0,97
1	DV736730		0,96
1	CU685349	Glutamine synthetase	0,96
1	AM861166	BTB/POZ domain-containing protein KCTD7	0,93
1	AM867241	Leucine-rich repeat serine/threonine-protein kise 1	0,95
1	AM856220		0,94
1	CU984090	Protein yellow	0,97
1	AM864486	Thymidylate synthase	0,88
1	BQ427051	Serine/threonine-protein kise PINK1, mitochondrial	0,93
1	AM860025	Uncharacterized protein C16orf48	0,92
1	CU992106	hypothetical protein CGI_10006558	0,80
1	AM853519		0,98
1	BQ427158		0,91
1	CU683033	WD repeat-containing protein 59	0,96
1	CU686177	fem-1-like protein A	0,93
1	CU998485	hypothetical protein CGI_10016002	0,97
1	FP000796		0,97
1	FP005545		0,86
1	FP003281	Tripartite motif-containing protein 2	0,97
2	CU997596	Serine/arginine repetitive matrix protein 1	1,02
2	EE677885		1,02
2	AM858007		1,06
2	CU684577	Nuclear receptor subfamily 2 group F member 1-A	1,10
2	AM860739		1,04
2	FP007294	Zinc transporter ZIP14	1,06
2	FD483982		1,09
2	AM867414	A disintegrin and metalloproteise	1,07
2	AM859478		1,12
2	AM860643		1,03
2	CU988648		1,05
2	AM858816		1,08
2	AM868839	Interferon-induced protein 44-like protein	1,23
2	AM856492	Histidine triad nucleotide-binding protein 1	1,13
2	CU992187	Regulator of telomere elongation helicase 1	1,04

Cluster	GenBank	Hit_Definition	Fold change
1	FP011368	ATPase family AAA domain-containing protein 2B	0,98
1	AM857228	Putative HERC2-like protein 3	0,96
1	CU989229		0,94
1	AM867174	V-type proton ATPase subunit B	0,94
1	AM857197	hypothetical protein CGI_10008389	0,93
1	ES789795	WD repeat-containing protein 66	0,94
1	AM867534	ALK tyrosine kinase receptor	0,79
1	FP006800		0,75
1	EX956372		0,74
1	FP007248	hypothetical protein CGI_10010145	0,75
1	EE677591		0,96
1	CU994914	hypothetical protein CGI_10016342	0,94
1	AM858882		0,94
1	AM865922		0,81
1	AM862485	Putative glutamyl-tRNA(Gln) amidotransferase subunit B	0,93
1	CU997780		0,77
1	CK172304	DNA replication licensing factor mcm5	0,95
1	DV736297		0,92
1	BQ427244	Anaphase-promoting complex subunit 10	0,92
1	ES789769		0,90
1	FP009233	Plasma membrane calcium-transporting ATPase 3	0,97
1	CU992435	RNA-binding protein 26	0,96
1	FP005411	hypothetical protein CGI_10005167	0,90
1	AM862326	Retinoblastoma-binding protein 6	0,94
1	CU998341		0,96
1	AM855240		0,95
1	AM864719		0,92
1	AM865006		0,86
1	AM858827	Protein lin-10	0,86
1	AM856185		0,81
1	CX069213	T-complex protein 1 subunit eta	0,93
1	AM860412		0,94
1	AM868805	hypothetical protein CGI_10022659	0,88
1	CU683708	Neurogenic locus Notch protein	0,95
1	AM854530	ADP-ribosylation factor-like protein 3	0,94
1	CU684156		0,95
1	AM858428		0,92
1	CF369211	hypothetical protein CGI_10028817	0,99
1	AM856027	Inactive ubiquitin carboxyl-terminal hydrolase 54	0,93
1	AM863972		0,88
1	EW778587	Poly [ADP-ribose] polymerase 14	0,93
2	ES789508	hypothetical protein CGI_10006610	1,14
2	CU995006		1,05
2	AM862099	H/ACA ribonucleoprotein complex non-core subunit NAF1	1,12
2	AM866255	Protein FAM8A1	1,12
2	AM859674	hypothetical protein CGI_10025437	1,04
2	EX956440		1,23
2	AM859011	Ubiquitin-conjugating enzyme E2 U	1,07
2	AM862592	Signal recognition particle receptor subunit alpha	1,04
2	CU987182	hypothetical protein CGI_10007367	1,05
2	AM856289	Pancreatic lipase-related protein 1	1,05
2	FP003635	hypothetical protein CGI_10000335	1,10
2	FP003781		1,03
2	AM857580		1,06
2	CU682163		1,03

2	FP000435	BolA-like protein 2	1,08
2	AM856629	hypothetical protein CGI_10017643	1,06
2	CU995974	E3 SUMO-protein ligase PIAS1	1,36
2	CU996409	Tenascin-R	1,07
2	AM868592		1,02
2	AM859873	Endoplasmic reticulum lectin 1	1,09
2	CU683027	Perlucin	1,09
2	AM855600	NADPH oxidoreductase A	1,13
2	AM856599	Calcyphosin-like protein	1,26
2	AM859679	Trafficking protein particle complex subunit 4	1,06
2	AM867888	Protein CBFA2T1	1,11
2	AM867452	Transcription factor RFX3	1,11
2	CU686583	Mitochondrial 2-oxoglutarate/malate carrier protein	1,06
2	DV736609	Yolk ferritin	1,12
2	FP000510		1,07
2	CU999045	Small nuclear ribonucleoprotein-associated protein B'	1,36
2	CU994551	Protein MEMO1	1,23
2	FP006590	hypothetical protein CGI_10007261	1,29
2	FP002017	hypothetical protein CGI_10007261	1,32
2	AM868784		1,06
2	ES789586	Puromycin-sensitive aminopeptidase	1,07
2	CB617457	Cathepsin L	1,15
2	CU990417	Actin-related protein 2/3 complex subunit 4	1,55
2	AM853726	Carboxypeptidase D	1,08
2	AM865792	RecQ-mediated genome instability protein 1	1,11
2	CU988288	Putative ferric-chelate reductase 1	1,02

Figure S6
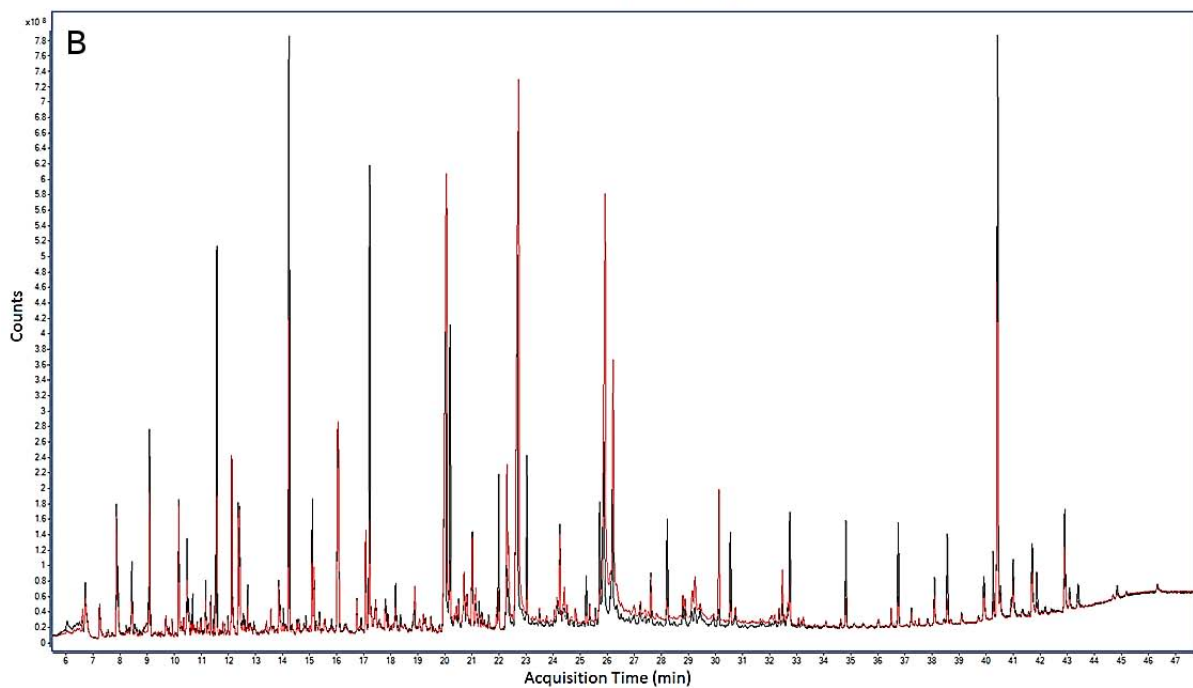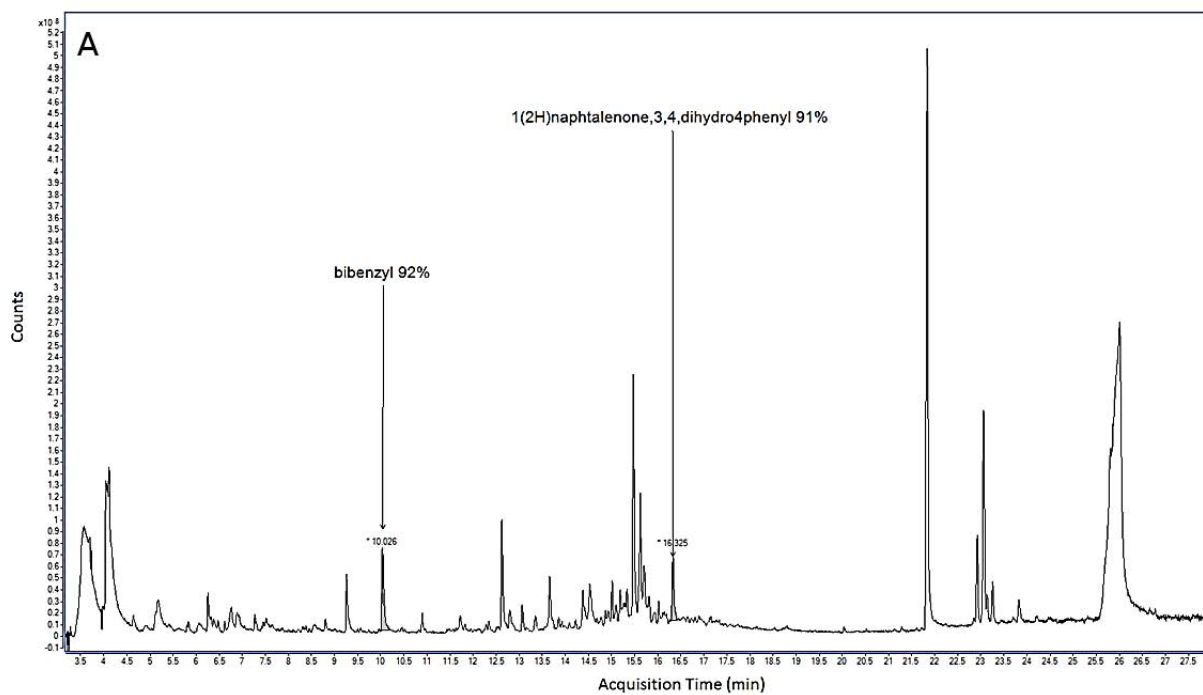
1   **Supplementary file 7.** Highest microplastic concentrations measured in nature and used in some experimental studies, including the present one.

Reference	*In situ* location or experiment [a]	Size	Plastic type and polymer [b]	Mass concentration in standard unit mg L^{-1}	Mass concentration in original unit [c]
[65]	California current system	> 333 µm	fragments	5.33	
[66]	South Pacific Gyre	> 333 µm	fragments, lines, films spheres,	0.073 [d]	732 g km^{-2}
[67]	North Pacific Central Gyre	> 333 µm	fragments, lines, films	3.02 [d]	30 169 g km^{-2}
[68]	Danube [e]	> 500 µm	pellets, flakes, spherules	0.697	
[69]	India, Sediment	> 0.45 µm	fragments, PU, PA, PS, PES	162 [f]	89 mg kg^{-1} dry weight
[10]	Exp, mussel	30 nm	spheres, PS	100-200-300	
[15]	Exp, mussel	1−80 µm	particles, HDPE	2500	
[17]	Exp, mussel	<100 µm	particles, PS, PE	1500	
[21]	Exp, *Daphnia*	~70 nm	spheres, PS	0.22-150	
this study	Exp, oyster	2 and 6 µm	spheres, PS	0.023	

2   [a] Exp. indicates experimental study, for which targeted species was added.

3   [b] PU polyurethane; PA polyamides (nylon); PS polystyrene; PES polyester; HDPE high-density polyethylene particle; PE polyethylene.

4   [c] When estimates in mg L^{-1} were calculated, original published data are given.

5   [d] For these two manta trawl samplings, mass concentration was estimated on reported concentrations in g km^{-2}, with an estimated trawling depth of 0.01 m, as

6   done by Besseling et al. [21].

7   [e] Estimated to directly enter the Black Sea, considered as a proxy of the concentration in the Danube estuary, where there are populations of wild oysters.

8   [f] A concentration in pore water of 162 mg L^{-1} was estimated by Besseling et al. [21], based on a mean concentration of 89 mg kg^{-1} dry sediment [69] and with

9   a sediment density of 2 kg L^{-1} and a water content of 50% on mass basis. This estimate can go up to 780 mg L^{-1} for the highest reported concentration in

10   sediment, *i.e.* 391 mg kg^{-1} dry sediment [70].